

1 **High-molecular-weight esters in α -pinene ozonolysis secondary organic aerosol:**
2 **Structural characterization and mechanistic proposal for their formation from highly**
3 **oxygenated molecules**

4 A. Kahnt^{1,a}, R. Vermeulen^{1,b}, Y. Iinuma^{2,c}, M. Safi Shalamzari^{1,d}, W. Maenhaut³, and M. Claeys¹

5
6 [1] Department of Pharmaceutical Sciences, University of Antwerp (Campus Drie Eiken), BE-2610, Antwerp,
7 Belgium

8 [2] Leibniz-Institut für Troposphärenforschung (TROPOS), Permoserstr. 15, D-04318 Leipzig, Germany

9 [3] Department of Chemistry, Ghent University, Krijgslaan 281, S12, BE-9000 Ghent, Belgium

10 [^a] now at: Development Bioanalysis, Janssen R&D, Turnhoutseweg 30, BE-2340 Beerse, Belgium

11 [^b] now at: Soil Service of Belgium, W. de Croylaan 48, BE-Heverlee, Belgium

12 [^c] now at: Okinawa Institute of Science and Technology Graduate University, 1919-1 Tancha, Onna-son,
13 Kunigami, Okinawa 904-0495 Japan

14 [^d] now at: Dr. Reddy's Laboratories Ltd., Zernikedreef 12, 2333 CL Leiden, The Netherlands

15 Correspondence to: M. Claeys (magda.claeys@uantwerpen.be)

16 **Abstract**

17 Stable high-molecular-weight esters are present in α -pinene ozonolysis secondary organic aerosol (SOA) with
18 the two most abundant ones corresponding to a diaterpenylic ester of *cis*-pinic acid with a molecular weight
19 (MW) of 368 (C₁₉H₂₈O₇) and a hydroxypinonyl ester of *cis*-pinic acid with a MW of 358 (C₁₇H₂₆O₈). However,
20 their molecular structures are not completely elucidated and their relationship with highly oxygenated
21 molecules (HOMs) in the gas phase is still unclear. In this study, liquid chromatography in combination with
22 positive ion electrospray ionization mass spectrometry has been performed on high-molecular-weight esters
23 present in α -pinene/O₃ SOA with and without derivatization into methyl esters. Unambiguous evidence could be
24 obtained for the molecular structure of the MW 368 ester in that it corresponds to an ester of *cis*-pinic acid
25 where the carboxyl substituent of the dimethylcyclobutane ring and not the methylcarboxyl substituent is
26 esterified with 7-hydroxypinonic acid. The same linkage was already proposed in previous work for the MW
27 358 ester (Yasmeen et al., 2010), but could be supported in the present study. Guided by the molecular
28 structures of these stable esters, we propose a formation mechanism from gas-phase HOMs that takes into

29 account the formation of an unstable $C_{19}H_{28}O_{11}$ product, which is detected as a major species in α -pinene
30 ozonolysis experiments as well as in the pristine forest atmosphere by chemical ionization – atmospheric
31 pressure ionization – time-of-flight mass spectrometry with nitrate clustering (Ehn et al., 2012, 2014). It is
32 suggested that an acyl peroxy radical related to *cis*-pinic acid ($RO_2\cdot$) and an alkoxy radical related to 7- or 5-
33 hydroxypinonic acid ($R'O\cdot$) serve as key gas-phase radicals and combine according to a $RO_2\cdot + R'O\cdot \rightarrow RO_3R'$
34 radical termination reaction. Subsequently, the unstable $C_{19}H_{28}O_{11}$ HOM species decompose through the loss of
35 oxygen or ketene from the inner part containing a labile trioxide function and the conversion of the unstable
36 acyl hydroperoxide groups to carboxyl groups, resulting in stable esters with a molecular composition of
37 $C_{19}H_{28}O_7$ (MW 368) and $C_{17}H_{26}O_8$ (MW 358), respectively. The proposed mechanism is supported by several
38 observations reported in the literature. On the basis of the indirect evidence presented in this study, we
39 hypothesize that $RO_2\cdot + R'O\cdot \rightarrow RO_3R'$ chemistry is at the underlying molecular basis of high-molecular-
40 weight ester formation upon α -pinene ozonolysis and may thus be of importance for new particle formation and
41 growth in pristine forested environments.

1 Introduction

The molecular characterization of secondary organic aerosol (SOA) has been a topic of interest in atmospheric chemistry for the last decades, owing to the importance of organic aerosol in air quality and climate (for a review, see Nozière et al., 2015). SOA comprises a large number of oxygenated organic compounds, is a major constituent of submicrometer atmospheric particulate matter (PM), and both biogenic (e.g., isoprene, monoterpenes, sesquiterpenes) and anthropogenic (aromatics, *n*-alkanes) volatile organic compounds (VOCs) serve as precursors for SOA. Abundant biogenic VOCs in the terrestrial atmosphere are monoterpenes, having an annual global emission rate of 155 Tg with α -pinene as the major terpene emitted (Guenther et al., 2012). Several multifunctional SOA compounds, including monomers and dimers from α -pinene oxidation have been structurally identified (for a review, see Nozière et al., 2015). Recently, “extremely low-volatility organic compounds” (ELVOCs), currently termed “highly oxygenated molecules” (HOMs), originating from α -pinene ozonolysis have been detected in both laboratory and field experiments by chemical ionization – atmospheric pressure ionization – time-of-flight (CI-APi-TOF) mass spectrometry with nitrate clustering (Ehn et al., 2012, 2014; Zhao et al., 2013) and have received much attention because of their role in driving new particle formation and growth in pristine forested environments. Molecular characterization of α -pinene SOA constituents is needed to elucidate the underlying formation mechanism and establish its link with gas-phase HOMs, and efforts in this direction have recently been undertaken (Mutzel et al., 2015; Zhang et al., 2015; Krapf et al., 2016; Zhang et al., 2017). However, the relationship of HOMs detected in the gas phase upon α -pinene ozonolysis with stable high-molecular-weight SOA constituents is unclear, so that there is still a missing element in closing the α -pinene SOA system.

High-molecular-weight esters have been reported in α -pinene/O₃ SOA but their detailed chemical structures are only partially elucidated and their mechanism of formation is still elusive. A high-molecular-weight compound with a molecular weight (MW) of 358 has been reported for the first time by Hofmann et al. (1998) in α -pinene/O₃ SOA using off- and online mass spectrometry (MS). With online atmospheric pressure chemical ionization (APCI) MS it was shown that this compound is formed concomitantly with two monomers, i.e., *cis*-pinic acid and a MW 172 compound that was tentatively identified as norpinic acid. Tandem MS on the deprotonated compound (*m/z* 357) revealed that it has a *cis*-pinic acid residue (*m/z* 185) as well as a *m/z* 171 residue. Later work by Müller et al. (2008) focused on the structure of the MW 368 compound. It was shown that this compound is composed of *cis*-pinic and hydroxypinonic acid parts, which are linked together by an ester bridge. The structure of the MW 358 compound was also addressed by Yasmeen et al. (2010), who revised the structure of this compound and presented evidence that it is a diaterpenylic ester of *cis*-pinic acid. The same conclusion was reached by Gao et al. (2010), who also showed that the MW 358 ester is a major product in α -

75 pinene ozonolysis experiments performed at low mass loadings. Recent work by Beck and Hoffmann (2016),
76 where use was made of derivatization to the *n*-butylesters and subsequent tandem MS analysis of the lithiated
77 and ammoniated molecules, supported the structure of the MW 358 ester as a diaterpenylic ester of *cis*-pinic
78 acid. Furthermore, the MW 358 ester was detected as a major tracer in β -pinene ozonolysis SOA
79 characterization studies (Iinuma et al., 2007; Yasmeen et al., 2010).

80 It is noted that prior to the studies by Müller et al. (2008) and Yasmeen et al. (2010) several studies dealt with
81 the molecular characterization of high-molecular-weight compounds and that very different possible structures
82 have been advanced. Gao et al. (2004) assigned the MW 358 α -pinene/O₃ compound to a dehydration product
83 formed between the gem-diol forms of two norpinonic acid molecules. Iinuma et al. (2004) reported MW 354
84 and 370 α -pinene/O₃ products that were enhanced in acidic conditions and tentatively assigned them to reaction
85 products between the gem-diol of pinonaldehyde and pinonaldehyde, and between pinonaldehyde and
86 hydroxypinonaldehyde, respectively. Docherty et al. (2005) proposed peroxydicarboxylic acid dimers for the
87 structure of higher-MW SOA products from the ozonolysis of α -pinene in which peroxydicarboxylic acid and the gem-
88 diol of a keto or aldehydic compound are connected via a peroxy bridge. Tolocka et al. (2004) characterized
89 high-molecular-weight compounds in α -pinene ozonolysis SOA and suggested that the products were most
90 likely formed by aldol and/or gem diol formation. In addition, Witkowski and Gierczak (2014) explained the
91 formation of MW 338 and 352 compounds in α -pinene ozonolysis as aldol reaction products of α -
92 acyloxyhydroperoxy aldehydes. All the above mentioned studies thus provide evidence that the structure
93 elucidation of high-molecular-weight α -pinene/O₃ compounds has turned out to be very challenging.

94 With regard to the structure elucidation of the MW 358 ester there is still ambiguity, in that two positional
95 isomers are possible (Fig. 1), and that different positional isomers have been proposed by Yasmeen et al. (2010)
96 [structure (a)], Gao et al. (2010) [structure (b)], and Beck and Hoffmann (2016) [structure (b)]. Based on the
97 MS data obtained it is not possible to unambiguously support the structure of one or the other positional isomer.
98 This issue will be further addressed in Section 3. The same ambiguity holds for the MW 368 ester (Fig. 1). In
99 addition to the MW 358 and 368 esters, minor high-molecular-weight compounds (i.e., MWs 272, 300, 308,
100 312, 314, 326, 338, 344, 352, 356, 376, 378 and 400) have also been reported in α -pinene/O₃ SOA (Müller et
101 al., 2008; Yasmeen et al., 2010; Kourtchev et al., 2014; Witkowski and Gierczak, 2014; Zhang et al., 2015) but
102 these products will not be addressed in the present paper.

103 High-molecular-weight esters have been detected up till now in many field studies that were conducted in
104 forested regions. MW 358 and 368 esters were first reported in ambient nighttime PM with an aerodynamic
105 diameter $\leq 2.5 \mu\text{M}$ (PM_{2.5}) that was collected at K-pusztá, Hungary, during a 2006 summer campaign (Yasmeen
106 et al., 2010). They were later detected in several field studies that were conducted in other forested

107 environments (Kristensen et al., 2013, 2016; Kourtchev et al., 2014, 2015). It was shown by Kourtchev et al.
108 (2016) that oligomers (i.e., hetero-oligomers) are of climatic relevance in that elevated SOA mass is one of the
109 key drivers of oligomer formation not only in laboratory experiments but also in the ambient atmosphere. It was
110 also demonstrated in the latter study that the oligomer content is strongly correlated with cloud condensation
111 nuclei activities of SOA particles. Furthermore, it could be demonstrated in laboratory chamber experiments
112 that the ratio monomers/oligomers and the oligomer content in α -pinene ozonolysis SOA are enhanced at low
113 temperature and low precursor concentrations, conditions that are relevant for the upper troposphere (Huang et
114 al., 2017).

115 Efforts to understand ester formation from α -pinene ozonolysis have also been actively undertaken. Yasmeen et
116 al. (2010) proposed that ester formation took place in the particle phase by esterification of *cis*-pinic acid with
117 terpenylic acid but this mechanism was not retained in later studies. Kristensen et al. (2014) demonstrated their
118 formation through gas-phase ozonolysis and supported the participation of a stabilized Criegee intermediate, as
119 previously suggested for the formation of unstable high-molecular-weight compounds that play a role in new
120 particle formation (Ziemann, 2002; Bonn et al., 2002; Lee and Kamens, 2005). In a study by Zhang et al.
121 (2015), the dynamics of particle-phase components of α -pinene SOA formation were investigated in detail. It
122 was shown that formation of monomeric products like *cis*-pinic acid is observed after the consumption of α -
123 pinene upon ozonolysis, which cannot be explained solely by a gas-phase mechanism and points to a particle-
124 phase mechanism. A mechanism involving gas-phase radical combination of acyl peroxy radicals and a
125 condensed-phase rearrangement was proposed that potentially explains the α -pinene SOA features in terms of
126 molecular structure, abundance, growth rates, evolution patterns, and responses to variations in temperature,
127 relative humidity, and oxidant type. Furthermore, a recent study by Zhang et al. (2017), using ozonolysis of
128 deuterium-labeled α -pinene, demonstrated that hydroperoxy derivatives of pinonic acid containing the
129 hydroperoxy group at different positions are components of HOMs that are present in the particle phase. In
130 work prior to the above cited investigations other studies already suggested the involvement of acyl peroxy
131 radicals in the formation of HOMs upon α -pinene ozonolysis (Ziemann, 2002; Docherty et al., 2005). In
132 addition, the suggestion that peroxy radicals are involved in the formation of dimers also fits to the observation
133 of a suppression of new particle formation from monoterpene oxidation by NO_x (Wildt et al., 2014).
134 Furthermore, evidence for peroxyhemiacetal formation upon α -pinene ozonolysis has also been reported (Hall
135 and Johnston, 2012a). All the above cited studies thus document that establishing the underlying molecular
136 mechanism leading to ester formation in α -pinene ozonolysis is challenging. This is mainly due to a lack of
137 knowledge (or only a partial knowledge, i.e., molecular formulae) of the molecular structures of both gas-phase
138 intermediates and particulate-phase end products.

139 In the present paper, we focus on the structural characterization of the MW 358 and 368 esters that are present
140 in α -pinene/O₃ SOA. To this aim, we have performed liquid chromatography/ electrospray ionization mass
141 spectrometry (LC/ESI-MS) in the positive ion mode on α -pinene/O₃ SOA with and without derivatization into
142 methyl esters. A soft methylation procedure using ethereal diazomethane was selected to avoid hydrolysis of the
143 ester function present in the targeted hetero-dimers. The aim of the methylation was two-fold: on the one hand,
144 to confirm the number of free carboxyl functions, and on the other hand, to obtain mass spectrometric
145 fragmentation that is different from that of intact esters in (+)ESI and to that obtained in previous studies on
146 intact esters in (-)ESI (Müller et al., 2008; Yasmeen et al., 2010; Zhang et al., 2015). Led by the molecular
147 structures of the MW 368 and MW 358 esters, we propose a formation mechanism that takes into account the
148 detection of a C₁₉ HOM in the gas phase by CI-APi-TOF MS with nitrate clustering (Ehn et al., 2012, 2014;
149 Zhao et al., 2013) and involves the combination of an acyl peroxy radical related to *cis*-pinic acid with an
150 alkoxy radical related to isomeric hydroxypinonic acids, which are, as *cis*-pinic acid, major monomers in α -
151 pinene SOA.

152 2. Experimental

153 2.1 α -pinene/O₃ chamber aerosol

154 Filter samples from α -pinene ozonolysis were obtained from experiments carried out in the 19 m³ TROPOS
155 aerosol chamber at 50% relative humidity and 21 °C. 1.6 ppm α -pinene was reacted with 615 ppb ozone without
156 seed particles and no OH radical scavenger was added. The aerosol formed was sampled after about one hour of
157 reaction time using a quartz fibre filter, and the sample was stored at -22 °C before analysis.

158 2.2 Filter sample preparation for analysis

159 A quarter of the chamber aerosol filter was extracted using three times 10 mL methanol and applying ultrasonic
160 agitation for 3 min. The combined extracts were concentrated to about 1 mL at 35 °C with a rotary evaporator,
161 were transferred to a 1 mL reaction glass vial, and were blown to dryness under a stream of nitrogen. The dried
162 residue was reconstituted in 250 μ L methanol/water (50/50, v/v) and analyzed by LC/(+)ESI-MS to characterize
163 the non-derivatized dimers. Another quarter of the filter was similarly extracted but was further subjected to a
164 methylation procedure using ethereal diazomethane to derivatize free carboxylic acids into their corresponding
165 methyl esters. Diazomethane was freshly prepared using the precursor diazald (99%, Sigma-Aldrich) according
166 to a standard procedure (Furniss et al., 1989). 500 μ L from the ethereal diazomethane solution was added to the
167 dried filter extract. After a reaction time of about 5 min, the sample was dried under a gentle stream of nitrogen
168 and reconstituted in 250 μ L methanol/water (50/50, v/v) for LC/(+)ESI-MS analysis of methylated compounds.

2.3 Chemical analysis

LC/ESI-MS analysis was carried out using a Surveyor Plus system (pump and autosampler) (Thermo Scientific, San Jose, CA, USA) and the chromatographic separation for both the non- and the derivatized filter extracts was performed on an Atlantis T3 column (2.1 x 150 nm, 3 μm particle size, Waters, Milford, MA, USA). An injection volume of 10 μL was used and a flow rate of 0.2 mL min^{-1} was applied. The mobile phases consisted of (A) 50 mM ammonium formate buffer with pH 3 and (B) methanol. A 65-min gradient was applied using the following program: (B) was kept at 3% for 5 min, increased to 95% in 15 min and kept for 25 min, followed by the reconditioning to 3% in 10 min and keeping (B) at 3% for 10 min. A linear ion trap mass spectrometer (LXQ, Thermo Scientific, San Jose, CA, USA) operated in the positive mode was used as the mass analyzer and details regarding operational and optimization procedures can be found in Kahnt et al. (2014). Under the LC conditions used, ammoniated adducts were detected owing to the presence of ammonium formate in mobile phase (A). The ion abundance ratios $[\text{M} + \text{NH}_4]^+ / [\text{M} + \text{H}]^+$ were 13.0, 15.6, 38 and 7.7, for the MW 358 ester, MW 368 ester, MW 358 ester trimethylated derivative and MW 368 ester dimethylated derivative, respectively. In the ion trap MS^n experiments, ammonia adducts were selected as precursor ions because these ions were more abundant than the protonated molecules and lose ammonia upon MS^2 , resulting in protonated molecules of which the fragmentation can be readily explained.

3. Results and Discussion

3.1. Characterization of the MW 358 and 368 high-molecular weight esters

3.1.1. Previous studies on $[\text{M} - \text{H}]^-$, $[\text{M} + \text{NH}_4]^+$ and $[\text{M} + \text{Li}]^+$ molecular species

For clarity, we summarize here selected MS data already reported in a previous study (Yasmeen et al., 2010) that led to the structural characterization of the MW 358 ester from α -pinene ozonolysis SOA as a diaterpenylic ester of *cis*-pinic acid. The data are given in Section 1 of the supplement (Fig. S1 and Scheme S1). Only one MW 358 isomer was detected in α -pinene/ O_3 SOA; upon MS^2 its deprotonated molecule $[\text{M} - \text{H}]^-$ fragments to product ions at m/z 185 and 171, which are attributed to *cis*-pinic and diaterpenylic acid, respectively. However, based on this information alone the ester linkage cannot be firmly established since two positional isomers are possible (Fig. 1). A minor MW 358 isomer was also detected in β -pinene ozonolysis SOA, which was very similar to that observed from α -pinene but showed an additional MS^2 $[\text{M} - \text{H}]^-$ product ion at m/z 189, which could best be explained with a positional isomeric structure [structure (b); Fig 1]. MS^2 data for the latter product are presented in Fig. S2 and Scheme S2 of the supplement. More recent work by Beck and Hoffmann (2016) involving fragmentation of lithiated and ammoniated molecular species of the *n*-butylated derivative supported the structure of the MW 358 ester from α -pinene/ O_3 SOA as a diaterpenylic ester of *cis*-pinic acid; however,

200 these authors suggested a positional isomeric structure [structure (b); Fig. 1] which is different from that
201 proposed by Yasmeeen et al. (2010) [structure (a); Fig. 1]. The MS data obtained for the $[M + \text{NH}_4]^+$ and $[M +$
202 $\text{Li}]^+$ molecular species of the *n*-butylated derivative also do not enable unambiguous differentiation between
203 positional isomeric structures.

204 For both the MW 358 and 368 esters accurate mass measurements to obtain the molecular compositions have
205 also been performed in previous studies using (-)ESI (e.g., Zhang et al., 2015), and are not repeated in the
206 present study. The molecular compositions of the MW 358 and 368 esters are $\text{C}_{17}\text{H}_{26}\text{O}_8$ and $\text{C}_{19}\text{H}_{28}\text{O}_7$,
207 respectively.

208 [Fig. 1]

209 3.1.2. Mass spectrometric behavior of the ammoniated underivatized MW 358 ester

210 LC chromatographic data obtained for underivatized α -pinene/ O_3 SOA are provided in Fig. S3 of the
211 supplement. It can be seen that the MW 358 product signal in both the negative (m/z 357) and positive ion mode
212 (m/z 376) has about half the intensity of the m/z 367 (MW 368) signal, and shows intensities in the same range
213 as the monomers detected at m/z 171 (MW 172; terpenylic acid), m/z 185 (MW 186; *cis*-pinic acid), and m/z
214 199 (MW 200; hydroxypinonic acids).

215 Selected LC/(+)ESI-MS data for the non-derivatized MW 358 ester with its proposed structure in α -pinene/ O_3
216 SOA are presented in Fig. 2 and Scheme 1. Fragmentation of the $[M + \text{NH}_4]^+$ leads to the loss of ammonia (m/z
217 359), yielding $[M + \text{H}]^+$, and further loss of a molecule of water (m/z 341), which can occur at different
218 positions. Abundant product ions are observed at m/z 173 and 187, which can be rationalized by processes
219 located in the internal ester linkage. The m/z 169 product ion can be explained through protonation of the ester
220 group (pathway a) or through a hydrogen rearrangement (pathway c) resulting in protonated *cis*-pinic acid (m/z
221 187) and subsequent loss of a molecule of water. However, it is noted that with a positional isomeric structure
222 product ions at the same m/z values could be expected. The m/z 173 ion results from protonation of the inner
223 ester group (pathway b) and can subsequently lose one or two molecules of water, giving rise to m/z 155 and
224 137, respectively. It can also be seen that m/z 155 can lead to the loss of CO giving rise to m/z 127. The m/z 169
225 ion fragments further through the loss of water, leading to m/z 151; here, we expect that the loss of water
226 proceeds more readily from structure (a) (Fig. 1) as water elimination from structure (b) would lead to strain in
227 the dimethylcyclobutane ring. We therefore retain structure (a) as the most likely structure for the major MW
228 358 ester present in α -pinene/ O_3 SOA.

229 [Fig. 2]

230 [Scheme 1]

231 3.1.3. Mass spectrometric behavior of the ammoniated MW 358 ester trimethylated derivative

232 LC chromatographic data obtained for methylated α -pinene/O₃ SOA are provided in Fig. S4 of the supplement.
233 It can be seen that the signal corresponding to the MW 358 ester detected at m/z 418 has a comparable intensity
234 as that corresponding to the MW 368 ester detected at m/z 414. The mass shifts observed due to derivatization
235 into methyl esters support that the MW 358 compound contains three carboxyl groups, while the MW 368
236 compound contains two such groups. The corresponding methylated monomers, i.e., terpenylic acid (detected at
237 m/z 204), *cis*-pinic acid (detected at m/z 232) and hydroxypinonic acid (detected at m/z 232) show intensities in
238 the same range as the methylated MW 358 and 368 esters.

239 Selected LC/(+)ESI-MS data for the derivatized MW 358 ester with its proposed structure in α -pinene/O₃ SOA
240 are presented in Fig. 3 and Scheme 2. Fragmentation of the $[M + NH_4]^+$ ion (m/z 418) leads to the formation of
241 three product ions at m/z 201, 169 and 141, while further fragmentation of m/z 201 upon MS³ mainly leads to
242 m/z 169, and MS⁴ of the generated m/z 169 mainly results in m/z 141. Two different structures can be proposed
243 for m/z 201; structure (a) can be explained following the loss of ammonia and ionization (protonation) at the
244 inner ester linkage, while structure (b) can be rationalized by a hydrogen rearrangement in the inner ester
245 linkage and loss of ammonia. Further loss of methanol (32 u) from m/z 201 results in m/z 169, with two possible
246 structures (c) and (d). It can be seen that structures (c) and (d) can give rise to the loss of CO, resulting in m/z
247 141. The weak ion at m/z 137 can be explained by fragmentation of m/z 169 [structure (c)] through loss of
248 methanol. It is noted that the same product ions could be explained from the positional isomeric structure of the
249 derivatized MW 358 ester; however, in this case we would expect a more abundant m/z 151 product ion, due to
250 a more favorable loss of water in the carboxymethyl terminus. Loss of a molecule of water from m/z 169
251 [structure (d)] leads to a weak product ion at m/z 151, while further loss of a molecule of ketene also results in
252 m/z 109.

253 [Fig. 3]

254 [Scheme 2]

255 3.1.4. Mass spectrometric behavior of the ammoniated underivatized MW 368 ester

256 Selected LC/(+)ESI-MS data for the ammoniated non-derivatized MW 368 ester with its proposed structure in
257 α -pinene/O₃ SOA are presented in Fig. 4 and Scheme 3. Fragmentation of the $[M + NH_4]^+$ upon MS² leads to
258 the loss of ammonia (m/z 369), yielding $[M + H]^+$, and product ions at m/z 351, 333, 307, 183 and 169, of which
259 m/z 351 is the base peak, and essentially the same pattern is seen upon MS³ of m/z 369. The product ions at m/z

260 351 and 333 in the higher mass range can simply be explained by the loss of one and two molecules of water,
261 respectively. The loss of CO₂ (44 u) leading to *m/z* 307 is difficult to explain from a carboxy terminus and likely
262 takes place from the inner ester linkage. The product ion at *m/z* 169 can be rationalized through protonation at
263 the inner ester function (route **a**) and further fragments through loss of water (*m/z* 151), as can be seen upon
264 MS³. Similarly, the product ion at *m/z* 183 can arise through protonation at the inner ester function (route **b**) and
265 further loss of water results in *m/z* 165. A positional isomeric structure (due to loss of water from the left
266 terminus) can also be suggested for *m/z* 351. The ions at *m/z* 169 and 183 can also occur after loss of water from
267 the left and right carboxyl terminus, respectively. It is noted that most ions discussed above can also be
268 explained with a positional isomeric structure [Fig. 1; structure (**a**)], although we would expect that such a
269 structure would lead to a less pronounced loss of water from *m/z* 369 resulting in *m/z* 351, as it would result in
270 strain in the dimethylcyclobutane ring. In addition, the formation of *m/z* 333, involving a second loss of water,
271 supports the proposed isomeric structure (**b**) (Fig. 1), as this process is more difficult to explain with isomeric
272 structure (**a**).

273 [Fig. 4]

274 [Scheme 3]

275 **3.1.5. Mass spectrometric behavior of the ammoniated MW 368 ester dimethylated derivative**

276 Selected LC/(+)ESI-MS data for the ammoniated MW 368 ester dimethyl derivative with its proposed structure
277 in α -pinene/O₃ SOA are presented in Fig. 5 and Scheme 4. Fragmentation of the [M + NH₄]⁺ (*m/z* 414) upon
278 MS² leads to the loss of ammonia (*m/z* 397), yielding [M + H]⁺, and product ions at *m/z* 379, 365, 269, 251,
279 201, 197, 183, 179, 165, 139 and 119, and essentially the same pattern is seen upon MS³ of *m/z* 397. The
280 product ions at *m/z* 379 and 365 in the higher mass range can simply be explained by the loss of a molecule of
281 water and methanol, respectively, of which the loss of water is due to an enolized keto group and that of
282 methanol can occur at one of the two methyl ester termini. The product ions at *m/z* 201 and 183, observed upon
283 MS² of *m/z* 414 and MS³ of *m/z* 397, can be explained through ionization at the inner ester linkage and a
284 hydrogen rearrangement. It is noted that these two product ions do not allow differentiating between positional
285 isomers of the MW 368 ester dimethyl derivative. The product ions at *m/z* 269 and 251, observed upon MS² of
286 *m/z* 414 and MS³ of *m/z* 397, can be explained by a cross-ring cleavage in the dimethylbutane ring, a
287 fragmentation that has been observed in previous studies for deprotonated *cis*-pinic acid (Yasmeen et al., 2011)
288 and deprotonated *cis*-norpinic acid (Yasmeen et al., 2010), both containing a keto group in α -position to the
289 dimethylcyclobutane ring. This fragmentation can be regarded as characteristic for one of the positional
290 isomeric forms, namely, structure (**b**) (Fig. 1), as it cannot be explained with the other positional isomeric form

291 (a). Further fragmentation upon MS³ of *m/z* 379 leads to *m/z* 251, 179 and 119, which can be rationalized by the
292 loss of propenoic acid (72 u), and the subsequent combined loss of methanol and carbon monoxide. Thus, the
293 MS data obtained for the ammoniated MW 368 ester dimethylated derivative unambiguously support structure
294 (b).

295 [Fig. 5]

296 [Scheme 4]

297 3.2. Possible formation mechanism for the MW 368 and MW 358 esters

298 3.2.1. General mechanistic considerations

299 It is noted that formation mechanisms involving unstable intermediates are generally hard to formulate as
300 unstable compounds cannot be isolated and structurally characterized; however, the molecular structure of the
301 gas-phase precursor (in this case, α -pinene), its known gas-phase chemistry, the molecular composition of
302 unstable intermediates and the molecular structure of stable end products observed in the particle phase can
303 provide crucial insights. Guided by the molecular structures of the MW 368 [Fig. 1; structure (b)] and MW 358
304 esters [Fig. 1; structure (a)] a formation mechanism is suggested, thereby taking into account that a C₁₉ HOM
305 has been detected as a major high-molecular-weight species in the gas phase upon α -pinene ozonolysis by CI-
306 APi-TOF MS with nitrate clustering (Ehn et al., 2012, 2014; Zhao et al., 2013; Krapf et al., 2016). It is noted
307 that the CI-APi-TOF MS technique does not reveal C₁₉ HOM species that correspond to direct analogues of the
308 MW 358 and 368 esters. In an effort to propose pathways that lead to the formation of the MW 368 and 358
309 esters, we have tried to formulate a uniform mechanism in that it involves the same acyl peroxy radical related
310 to *cis*-pinic acid and an alkoxy radical related to isomeric hydroxypinonic acids.

311 3.2.2. Formation mechanism proposed for the MW 368 ester

312 A possible formation mechanism leading to the MW 368 ester is outlined in Scheme 5. It is suggested that an
313 alkoxy radical related to 7-hydroxypinonic acid (a) (*cis*-2,2-dimethyl-3-hydroxyacetylcyclobutylethanoic acid;
314 for labeling, see Scheme S3 of the supplement) (R'O \cdot) and an acyl peroxy radical related to *cis*-pinic acid (b)
315 (RO₂ \cdot) serve as key intermediates. Radical termination according to a RO₂ \cdot + R'O \cdot \rightarrow RO₃R' reaction leads to a
316 HOM with a molecular composition of C₁₉H₂₈O₁₁ (c), which corresponds to a major gas-phase species upon α -
317 pinene ozonolysis (Ehn et al., 2012, 2014; Krapf et al., 2016). The proposed mechanism is inspired by the
318 mechanism suggested by Zhang et al. (2015) to explain the formation of a MW 326 ester, where two peroxy
319 radicals related to *cis*-pinic acid combine according to a RO₂ \cdot + RO₂ \cdot \rightarrow ROOR + O₂ reaction. Further
320 degradation of C₁₉H₂₈O₁₁ (c) involving the labile inner part containing a linear trioxide bridge through the loss

321 of oxygen and conversion of the acyl hydroperoxide groups to carboxyl groups results in the MW 368 ester
322 [Fig. 1; structure (b)] with a molecular composition of C₁₉H₂₈O₇ (d). It is noted that the formation of C₁₉H₂₈O₇
323 corresponds to a RO₂· + R'O· → ROR' + O₂ reaction, bearing similarity with the RO₂· + RO₂· → ROOR + O₂
324 reaction where the R groups are alkyl peroxy groups, which is known to involve a tetroxide intermediate (e.g.,
325 Bohr et al., 1999). As to the formation of a linear trioxide intermediate (c), trioxides containing a –(C=O)OOO–
326 function have been reported in the literature, e.g. tertiary alkyl peroxy hydrogen phthalates have been
327 synthesized and are used as catalysts for the polymerization of vinyl compounds (Komai, 1971). Unstable
328 intermediates formed from species (c) can also be considered, owing to the conversion of one acyl hydroperoxy
329 group (C₁₉H₂₈O₁₀), the conversion of two acyl hydroperoxy groups (C₁₉H₂₈O₉), the loss of oxygen (C₁₉H₂₈O₉),
330 and the loss of oxygen combined with the conversion of one acyl hydroperoxy group (C₁₉H₂₈O₈). In this
331 context, such species have been detected in the gas phase by CI-APi-TOF MS with nitrate clustering in an α-
332 pinene ozonolysis flow tube experiment by Krapf et al. (2016). The alternative mechanism leading to C₁₉H₂₈O₁₁
333 (c) involving an acyloxy radical related to *cis*-pinic acid and an alkyl peroxy radical related to 7-hydroxypinonic
334 acid is also theoretically possible but is not likely because of the mesomeric stabilization in the acyloxy radical.

335 [Scheme 5]

336 With regard to the suggestion that an alkoxy radical related to 7-hydroxypinonic acid is a key gas-phase radical,
337 it should be noted that hydroxypinonic acids are major monomers in α-pinene/O₃ SOA (Fig. S3). The detailed
338 mechanism leading to the peroxy radical related to *cis*-pinic acid (RO₂·) and the alkoxy radical related to 7-
339 hydroxypinonic acid (R'O·) are given in Scheme S4 of the supplement. The proposed RO₂· + R'O· → RO₃R'
340 radical termination reaction leads to a MW 368 ester with structure (b) (Fig. 1) [species (d) in Scheme 5],
341 namely, an ester of *cis*-pinic acid where the carboxyl substituent of the dimethylcyclobutane ring and not the
342 carboxymethyl group is esterified with 7-hydroxypinonic acid. It can also be seen that the labile gas-phase
343 intermediate (c) contains *cis*-pinic acid and 7-hydroxypinonic acid residues and thus can serve as a precursor for
344 these monomers and their corresponding hydroperoxides. In this context, a recent study by Zhang et al. (2017)
345 provided evidence for the formation of 7-hydroperoxypinonic acid from degradation of an unstable dimer
346 precursor in α-pinene/O₃ SOA. It is also worth mentioning that both *cis*-pinic acid (e.g., Yu et al., 1999; Glasius
347 et al., 2000; Larsen et al., 2001; Winterhalter et al., 2003) and 7-hydroxypinonic acid (e.g., Glasius et al., 1999;
348 Larsen et al., 2001; Yasmeen et al., 2012) are known to be present in α-pinene/O₃ SOA. The proposed
349 mechanism is consistent with the observation made by Zhang et al. (2015) that *cis*-pinic acid is still generated
350 after consumption of α-pinene upon ozonolysis, suggesting a particle-phase production pathway. It is also in
351 agreement with observations made by Lopez-Hilfiker et al. (2015) and Huang et al. (2017), who examined the
352 thermal behavior of α-pinene/O₃ SOA and found that *cis*-pinic acid and hydroxypinonic acid can also arise from

353 thermal decomposition of unstable hetero-oligomers. In addition, it is consistent with the findings by Mutzel et
354 al. (2015) that intact HOMs detected in the gas phase are carbonyl-containing compounds. Recent work has also
355 established that hydroperoxides present in α -pinene/O₃ SOA are unstable and quickly convert to more stable
356 products (Krapf et al., 2016). Furthermore, monomers including *cis*-pinic acid and terpenylic acid were found to
357 be major constituents of the 10 and 20 nm particles from α -pinene ozonolysis in a flow reactor (Winkler et al.,
358 2012), which are likely fragments of high-molecular-weight compounds due to the thermal decomposition of
359 unstable hetero-oligomers during resistive heating of particles in the thermal desorption chemical ionization MS
360 measurements (Hall and Johnston, 2012b).

361 3.2.3. Formation mechanism proposed for the MW 358 ester

362 A possible formation mechanism leading to the MW 358 ester is provided in Scheme 6. Compared to the
363 mechanism proposed for the MW 368 ester, an alkoxy radical related to 5-hydroxypinonic acid instead of an
364 alkoxy radical related to 7-hydroxypinonic acid participates in the $\text{RO}_2\cdot + \text{R}'\text{O}\cdot \rightarrow \text{RO}_3\text{R}'$ radical termination
365 reaction. The detailed mechanism leading to the alkoxy radical related to 5-hydroxypinonic acid is given in
366 Scheme S4 of the supplement. It is noted that the C₁₉H₂₈O₁₁ dimeric HOM species is a positional isomer of that
367 implicated in the formation of the MW 368 ester (Scheme 5). With regards to the suggestion that an isomeric
368 alkoxy radical is involved, a recent study by Zhang et al. (2017) provided evidence for the formation of the
369 corresponding hydroperoxy product, 5-hydroperoxypinonic acid, in α -pinene/O₃ SOA. As mentioned above,
370 hydroxypinonic acids are major monomers in α -pinene/O₃ SOA (Fig. S3), and it can be seen that at least two
371 positional isomeric hydroxypinonic acids are present. To arrive at the formation of the MW 358 ester [Fig. 1;
372 structure (a)], a complex rearrangement involving the labile inner part containing a linear trioxide function has
373 to be invoked. A detailed rearrangement mechanism is provided in Scheme S5 of the supplement. It can also be
374 seen that the labile intermediate (c) (Scheme 6) can serve as a precursor for *cis*-pinic acid, as it contains a *cis*-
375 pinic acid residue. In addition, it can be explained that this labile intermediate can also give rise to the formation
376 of terpenylic acid, a major monomer observed in α -pinene/O₃ SOA (Fig. S3) (Claeys et al., 2009) but here again
377 a complex rearrangement has to be invoked (Scheme S6 of the supplement). In this context, there is evidence
378 that unstable hetero-oligomers present in α -pinene/O₃ SOA produce terpenylic acid upon heating (Lopez-
379 Hilfiker et al., 2015). As already mentioned above, terpenylic acid was also found to be a major constituent of
380 the 10 and 20 nm particles from α -pinene ozonolysis in a flow reactor (Winkler et al., 2012), which is likely
381 formed by decomposition of unstable hetero-oligomeric species in the thermal desorption chemical ionization
382 MS measurements (Hall and Johnston, 2012b).

383 [Scheme 6]

4. Conclusions and atmospheric implications

Unambiguous mass spectrometric evidence has been obtained in this study for the linkage in the MW 368 ($C_{19}H_{28}O_7$) hydroxypinonyl ester of *cis*-pinic acid, which is an abundant compound present in α -pinene/ O_3 SOA; more specifically, the MW 368 compound corresponds to an ester of *cis*-pinic acid where the carboxyl substituent of the dimethylcyclobutane ring and not the methylcarboxyl substituent is esterified with 7-hydroxypinonic acid. This linkage was already proposed in previous work for the MW 358 ($C_{17}H_{26}O_8$) diaterpenylic ester of *cis*-pinic acid, another major compound present in α -pinene/ O_3 SOA (Yasmeen et al., 2010), but could be supported in the present study. Guided by the molecular structures of these stable esters, we propose a formation mechanism from highly oxygenated molecules in the gas phase that takes into account the detection of an unstable $C_{19}H_{28}O_{11}$ HOM as a major species by CI-APi-TOF MS with nitrate clustering (Ehn et al., 2012, 2014; Zhao et al., 2013; Krapf et al., 2016). It is suggested that an acyl peroxy radical related to *cis*-pinic acid ($RO_2\cdot$) and an alkoxy radical related to 7- or 5-hydroxypinonic acid ($R'O\cdot$) serve as key gas-phase radicals and combine according to a $RO_2\cdot + R'O\cdot \rightarrow RO_3R'$ radical termination reaction. Subsequently, the unstable $C_{19}H_{28}O_{11}$ dimeric HOM species decompose by the loss of oxygen or ketene from the inner part containing a labile linear trioxide bridge and the conversion of the unstable acyl hydroperoxide groups to carboxyl groups, resulting in stable esters with a molecular composition of $C_{19}H_{28}O_7$ (MW 368) and $C_{17}H_{26}O_8$ (MW 358), respectively. The proposed mechanism is supported by several observations reported in the literature, one of them being that *cis*-pinic acid is still generated after the consumption of α -pinene upon ozonolysis, suggesting its formation from an unstable HOM species (Zhang et al., 2015).

Further theoretical investigations are warranted to examine the proposed mechanism leading to the MW 368 and 358 esters present in α -pinene/ O_3 SOA. The mechanism is assumed to be energetically favorable as small stable molecules such as oxygen and ketene are expelled and a stable ester bridge is generated. The mechanism involves the combination of an acyl peroxy with an alkoxy radical according to a $RO_2\cdot + R'O\cdot \rightarrow RO_3R'$ reaction and thus differs from that proposed to explain the formation of a MW 326 ester, where two acyl peroxy radicals related to *cis*-pinic acid combine according to a $RO_2\cdot + RO_2\cdot \rightarrow ROOR + O_2$ reaction (Zhang et al., 2015). We hypothesize that $RO_2\cdot + R'O\cdot \rightarrow RO_3R'$ chemistry is at the underlying molecular basis of high-molecular-weight hetero-dimer formation in the gas phase upon α -pinene ozonolysis and may thus be of importance for new particle formation and growth in pristine forested environments.

Acknowledgements

Research at the University of Antwerp and TROPOS was supported by the Belgian Federal Science Policy Office through the network project "Biogenic Influence on Oxidants and Secondary Organic Aerosol:

415 theoretical, laboratory and modelling investigations (BIOSOA)". Research at the University of Antwerp was
416 also supported by the Research Foundation – Flanders (FWO), whereas research at TROPOS was also
417 supported by the European Commission through the EUROCHAMP-2 project (228335). We also would like to
418 thank Anke Mutzel, Torsten Berndt and Hartmut Herrmann from TROPOS for valuable discussions on the
419 proposed mechanism, and Olaf Böge for his help in the preparation of the α -pinene/O₃ SOA sample.

420 **Supplementary material related to this article is available online at <http://www.atmos-chem-phys.xxxx>.**

421 **References**

422 Beck, M. and Hoffmann, Th.: A detailed MSⁿ study for the molecular identification of a dimer formed from
423 oxidation of pinene, *Atmos. Environ.*, 130, 120-126, 2016.

424
425 Bohr., F., Henon, E., Garcia., I., and Castro., M.: Theoretical study of the peroxy radicals RO₂ self-reaction:
426 Structures and stabilization energies of the intermediate RO₄R for various R, *Int. J. Quantum Chem.*, 75, 671–
427 682, 1999.

428
429 Bonn, B., Schuster, G., and Moortgat, G.: Influence of water vapor on the process of new particle formation
430 during monoterpene ozonolysis, *J. Phys. Chem. A*, 106, 2869–2881, 2002.

431
432 Claeys, M., Iinuma, Y., Szmigielski, R., Surratt, J. D., Blockhuys, F., Van Alsenoy, C., Böge, O., Sierau, B.,
433 Gómez-González, Y., Vermeylen, R., Van der Veken, P., Shahgholi, M., Chan, A. W. H., Herrmann, H.,
434 Seinfeld, J. H., and Maenhaut, W.: Terpenylic acid and related compounds from the oxidation of α -pinene:
435 Implications for new particle formation and growth above forests, *Environ. Sci. Technol.*, 43, 6976–6982, 2009.

436
437 Ehn, M., Kleist, E., Junninen, H., Petäjä, T., Lönn, G., Schobesberger, S., Dal Maso, M., Trimborn, A.,
438 Kulmala, M., Worsnop, D. R., Wahner, A., Wildt, J., and Mentel, Th. F.: Gas phase formation of extremely
439 oxidized pinene reaction products in chamber and ambient air, *Atmos. Chem. Phys.*, 12, 5113–5127,
440 doi:10.5194/acp-12-5113, 2012.

441 Ehn, M., Thornton, J. A., Kleist, E., Sipilä, M., Junninen, H., Pullinen, I., Springer, M., Rubach, F., Tillmann,
442 R., Lee, B., Lopez-Hilfiker, F., Andres, S., Ismail-Hakki, A., Rissanen, M., Jokinen, T., Schobesberger, S.,
443 Kangasluoma, J., Kontkanen, J., Nieminen, T., Kurtén, T., Nielsen, L. B., Jørgensen, S., Kjaergaard, H. G.,
444 Canagaratna, M., Dal Maso, M., Berndt, T., Petäjä, T., Wahner, A., Kerminen, V.-M., Kulmala, M., Worsnop,

445 D. R., Wildt, J., and Mentel, Th. F.: A large source of low-volatility secondary organic aerosol, *Nature*, 506,
446 476–479, 2014.

447 Docherty, K. S., Wu, W., Lim, Y. B., and Ziemann, P. J.: Contributions of organic peroxides to secondary
448 aerosol formed from reactions of monoterpenes with O₃, *Environ. Sci. Technol.*, 39, 4049–4059, 2005.

449 Furniss, B. S., Hannaford, A. J., Smith, P. W. G., and Tatchell, A. R.: *Vogel's Textbook of Practical Organic*
450 *Chemistry*; John Wiley: New York, 1989.

451 Gao, S., Ng, N. L., Keywood, M., Varutbangkul, V., Bahreini, R., Nenes, A., He, J., Yoo, K. Y., Beauchamp, J.
452 L., Hodyss, R., Flagan, R. C., and Seinfeld, J. H.: Particle phase acidity and oligomer formation in secondary
453 organic aerosol, *Environ. Sci. Technol.*, 38, 6582–6589, 2004.

454 Gao, Y., Hall, W.A., and Johnston, M. V.: Molecular composition of monoterpene secondary organic aerosol at
455 low mass loading, *Environ. Sci. Technol.*, 44, 7897–7902, 2010.

456 Glasius, M., Duane, M., and Larsen, B. R.: Determination of polar terpene oxidation products in aerosols by
457 liquid chromatography–ion trap mass spectrometry, *J. Chrom. A*, 833, 121–135, 1999.

458 Glasius, M., Lahaniati, M., Calogirou, A., Di Bella, D., Jensen, N. R., Hjorth, J., Kotzias, D., and Larsen, B. R.:
459 Carboxylic acids in secondary aerosols from oxidation of cyclic monoterpenes by ozone, *Environ. Sci.*
460 *Technol.*, 34, 1001–1010, 2000.

461 Guenther, A. B., Jiang, X., Helad, C. L., Sakulyanontvittaya, T., Duhl, T., Emmons, L. K., and Wang, X.: The
462 Model of Emissions of Gases and Aerosols from Nature version 2.1 (MEGAN2.1): an extended and updated
463 framework for modeling biogenic emissions, *Geosci. Model Dev.*, 5, 1471–1492, 2012.

464 Hall, W. A. and Johnston, M. V.: Oligomer formation pathways in secondary organic aerosol from MS and
465 MS/MS measurements with high mass accuracy and resolving power, *J. Am. Soc. Mass Spectrom.*, 23, 1097–
466 1108, 2012a.

467 Hall, W. A. and Johnston, M. V.: The thermal-stability of oligomers in alpha-pinene secondary organic aerosol,
468 *Aerosol Sci. Technol.*, 46, 983–989, 2012b.

469 Hoffmann, T., Bandur, R., Marggraf, U., and Linscheid, M.: Molecular composition of organic aerosols formed
470 in the alpha-pinene/O₃ reaction: Implications for new particle formation processes, *J. Geophys. Res.*, 103,
471 25569–25578, 1998.

472 Huang, W., Saathof, H., Pajunoja, A., Shen, X., Naumann, K.-H., Wagner, R., Virtanen, A., Leisner, T., and
473 Mohr, C.: α -pinene secondary organic aerosol at low temperature: Chemical composition and implications for
474 particle viscosity, *Atmos. Chem. Phys. Discuss.*, <https://doi.org/10.5194/acp-2017-793>, 2017.
475

476 Iinuma, Y., Böge, O., Gnauk, T., and Herrmann, H.: Aerosol chamber study of the α -pinene/O₃ reaction:
477 influence of particle acidity on aerosol yields and products, *Atmos. Environ.*, 38, 761–773, 2004.

478 Iinuma, Y., Müller, C., Berndt, T., Böge, O., Claeys, M., and Herrmann, H.: Evidence for the existence of
479 organosulfates from beta-pinene ozonolysis in ambient secondary organic aerosol, *Environ. Sci. Technol.*, 41,
480 6678–6683, 2007.

481 Kahnt, A., Iinuma, Y., Mutzel, A., Böge, O., Claeys, M., and Herrmann, H.: Campholenic aldehyde ozonolysis:
482 a mechanism leading to specific biogenic secondary organic aerosol constituents, *Atmos. Chem. Phys.*, 14,
483 719–736, 2014.

484 Komai, T., Water-soluble tertiary-alkylperoxy hydrogen phthalates, *Jpn. Tokkyo Koho*, Patent, 1971.

485 Kourtchev, I., Fuller, S. J., Giorio, C., Healy, R. M., Wilson, E., O'Connor, I., J. C. Wenger, J. C., McLeod, M.,
486 Aalto, J., Ruuskanen, T. M., Maenhaut, W., Jones, R., Venables, D. S., Sodeau, J. R., Kulmala, M., and
487 Kalberer, M.: Molecular composition of biogenic secondary organic aerosols using ultrahigh-resolution mass
488 spectrometry: Comparing laboratory and field studies, *Atmos. Chem. Phys.*, 14, 2155–2167, 2014.

489 Kourtchev, I., Doussin, J.-F., Giorio, C., Mahon, B., Wilson, E. M., Maurin, N., Pangui, E., Venables, D. S.,
490 Wenger, J. C., and Kalberer, M.: Molecular composition of fresh and aged secondary organic aerosol from a
491 mixture of biogenic volatile compounds: A high-resolution mass spectrometry study, *Atmos. Chem. Phys.*, 15,
492 5683–5695, 2015.

493 Kourtchev, I., Giorio, C., Manninen, A., Wilson, E., Mahon, B., Aalto, J., Kajos, M., Venable, D., Ruuskanen,
494 T., Levula, J., Loponen, M., Connors, S., Harris, N., Zhao, D., Kiendler-Scharr, A., Mentel, T., Rudich, Y.,
495 Hallquist, M., Doussin, J.-F., Maenhaut, W., Bäck, J., Petäjä, T., Wenger, J., Kulmala, M., and Kalberer, M.:
496 Enhanced volatile organic compounds emissions and organic aerosol mass increase the oligomer content of
497 atmospheric aerosols, *Sci. Rep.*, 6:35038, doi:10.1038/srep35038, 2016.

498 Krapf, M., El Haddad, I., Bruns, E. A., Molteni, U., Daellenbach, K. R., Prévôt, A. S. H., Baltensperger, U., and
499 Dommen, J.: Labile peroxides in secondary organic aerosol, *Chem.*, 1, 603–616, 2016.

500 Kristensen, K., Enggrob, K. L., King, S. M., Worton, D. R., Platt, S. M., Mortensen, R., Rosenoern, T., Surratt,
501 J. D., Bilde, M., Goldstein, A. H., and Glasius, M.: Formation and occurrence of dimer esters of pinene
502 oxidation products in atmospheric aerosols, *Atmos. Chem. Phys.*, 13, 3763–3776, 2013.

503 Kristensen, K., Cui, T., Zhang, H., Gold, A., Glasius, M., and Surratt, J. D.: Dimers in α -pinene secondary
504 organic aerosol: effect of hydroxyl radical, ozone, relative humidity and aerosol acidity, *Atmos. Chem. Phys.*,
505 14, 4201–4218, 2014.

506 Kristensen, K., Watne, Å. K., Hammes, J., Lutz, A., Petäjä, T., Hallquist, M., Bilde, M., and Glasius, M.: High-
507 molecular weight dimer esters are major products in aerosols from α -pinene ozonolysis and the boreal forest,
508 *Environ. Sci. Technol. Lett.*, 3, 280–285, 2016.

509 Larsen, B. R., Di Bella, D., Glasius, M., Winterhalter, R., Jensen, N. R., and Hjorth, J.: Gas-phase OH oxidation
510 of monoterpenes: gaseous and particulate products, *J. Atmos. Chem.*, 38, 231–276, 2001.

511 Lee, S. and Kamens, R. M.: Particle nucleation from the reaction of α -pinene and O₃, *Atmos. Environ.*, 39,
512 6822–6832, 2005.

513 Lopez-Hilfiker, F. D., Mohr, C., Ehn, M., Rubach, F., Kleist, E., Wildt, J., Mentel, T. F., Carrasquillo, A. J.,
514 Daumit, K. E., Hunter, J. F., Kroll, J. H., Worsnop, D. R., and Thornton, J. A.: Phase partitioning and volatility
515 of secondary organic aerosol components formed from α -pinene ozonolysis and OH oxidation: the importance
516 of accretion products and other low volatility compounds, *Atmos Chem Phys*, 15, 7765–7776, 2015.

517 Müller, L., Reinnig, M.-C., Warnke, J., and Hoffmann, Th.: Unambiguous identification of esters as oligomers
518 in secondary organic aerosol formed from cyclohexene and cyclohexene/ α -pinene ozonolysis, *Atmos. Chem.*
519 *Phys.*, 8, 1423–1433, doi:10.5194/acp-8-1423-2008, 2008.

520 Mutzel, A., Poulain, L., Berndt, T., Iinuma, Y., Rodigast, M., Böge, O., Richters, S., Spindler, G., Sipilä, M.,
521 Jokinen, T., Kulmala, M., and Herrmann, H.: Highly oxidized multifunctional organic compounds observed in
522 tropospheric particles: A field and laboratory study, *Environ. Sci. Technol.*, 49, 7754–7761, 2015.

523 Nozière, B., Kalberer, M., Claeys, M., Allan, J., D’Anna, B., Decesari, S., Finessi, E., Glasius, M., Grgić, I.,
524 Hamilton, J. F., Hoffmann, T., Iinuma, Y., Jaoui, M., Kahnt, A., Kampf, C. J., Kourtchev, I., Maenhaut, W.,
525 Marsden, N., Saarikoski, S., Schnelle-Kreis, J., Surratt, J. D., Szidat, S., Szmigielski, R., and Wisthaler, A.: The
526 molecular identification of organic compounds in the atmosphere: State of the art and challenges, *Chem. Rev.*,
527 115, 3919–3983, 2015.

528 Tolocka, M. P., Jang, M., Ginter, J. M., Cox, F. J., Kamens, R. M., and Johnston, M. V.: Formation of
529 oligomers in secondary organic aerosol, *Environ. Sci. Technol.*, 38, 1428–1434, 2004.

530 Wildt, J., Mentel, T. F., Kiendler-Scharr, A., Hoffmann, T., Andres, S., Ehn, M., Kleist, E., M \ddot{u} sgen, P., Rohrer,
531 F., Rudich, Y., Springer, M., Tillmann, R., and Wahner, A.: Suppression of new particle formation from
532 monoterpene oxidation by NO $_x$, *Atmos. Chem. Phys.*, 14, 2789–2804, 2014.

533 Winkler, P. M., Ortega, J., Karl, T., Cappellin, L., Friedli, H. R., Barsanti, K., McMurry, P. H., and Smith, J. N.:
534 Identification of the biogenic compounds responsible for size-dependent nanoparticle growth, *Geophys. Res.*
535 *Lett.*, 39, L20815, doi:10.1029/2012GL053253, 2012.

536 Winterhalter, R., Van Dingenen, R., Larsen, B. R., Jensen, N. R., and Hjorth, J.: LC-MS analysis of aerosol
537 particles from the oxidation of α -pinene by ozone and OH-radicals, *Atmos. Chem. Phys. Discuss.*, 3, 1–39,
538 2003.

539 Witkowski, B. and Gierczak, T.: Early stage composition of SOA produced by α -pinene/ozone reaction: α -
540 Acyloxyhydroperoxy aldehydes and acidic dimers, *Atmos. Environ.*, 95, 59–70, 2014.

541 Yasmeeen, F., Vermeylen, R., Szmigielski, R., Iinuma, Y., B \ddot{o} ge, O., Herrmann, H., Maenhaut, W., and Claeys,
542 M.: Terpenylic acid and related compounds: precursors for dimers in secondary organic aerosol from the
543 ozonolysis of α - and β -pinene, *Atmos. Chem. Phys.*, 10, 9383–9392, doi:10.5194/acp-10-9383-2010, 2010.

544 Yasmeeen, F., Szmigielski, R., Vermeylen, R., G \acute{o} mez-Gonz \acute{a} lez, Y., Surratt, J. D., Chan, A. W. H., Seinfeld, J.
545 H., Maenhaut, W., and Claeys, M.: Mass spectrometric characterization of isomeric terpenoic acids from the
546 oxidation of α -pinene, β -pinene, *d*-limonene, and Δ^3 -carene in fine forest aerosol, *J. Mass Spectrom.*, 46, 425–
547 442, 2011.

548 Yasmeeen, F., Vermeylen, R., Maurin, N., Perraudin, E., Doussin, J.-F., and Claeys, M.: Characterisation of
549 tracers for aging of α -pinene secondary organic aerosol using liquid chromatography/negative ion electrospray
550 ionisation mass spectrometry, *Environ. Chem.*, 9, 236–246, 2012.

551 Yu, J., Cocker III, D. R., Griffin, R. J., Flagan, R. C., and Seinfeld, J. H.: Gas-phase ozone oxidation of
552 monoterpenes: Gaseous and particulate products, *J. Atmos. Chem.*, 34, 207–258, 1999.

553 Zhang, X., McVay, R. C., Huang, D. D., Dalleska, N. F., Aumont, B., Flagan, R. C., and Seinfeld, J. H.:
554 Formation and evolution of molecular products in α -pinene secondary organic aerosol, *Proc. Natl. Acad. Sci. U.*
555 *S. A.*, 112, 14168–14173, 2015.

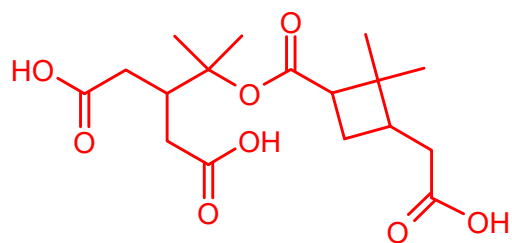
556 Zhang, X., Lambe, A. T., Upshur, M. A., Brooks, W. A., Gray Bé, A., Thomson, R. J., Geiger, F. M., Surratt, J.
557 D., Zhang, Z., Gold, A., Graf, S., Cubison, M. J., Groessl, M., Jayne, J. T., Worsnop, D. R., and Canagaratna,
558 M. R.: Highly oxygenated multifunctional compounds in α -pinene secondary organic aerosol, *Environ. Sci.*
559 *Technol.*, 51, 5932–5940, 2017.

560 Zhao, J., Ortega, J., Chen, M., McMurry, P. H., and Smith, J. N.: Dependence of particle nucleation and growth
561 on high-molecular-weight gas-phase products during ozonolysis of
562 α -pinene, *Atmos. Chem. Phys.*, 13, 7631–7644, 2013.

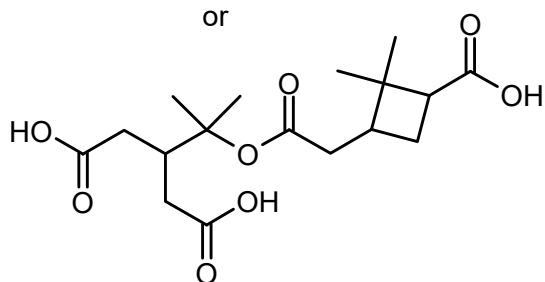
563 Ziemann, P. J.: Evidence for low-volatility diacyl peroxides as a nucleating agent and major component of
564 aerosol formed from reactions of ozone with cyclohexene and homologous compounds, *J. Phys. Chem. A*, 106,
565 4390–4402, 2002.

MW 358 (C₁₇H₂₆O₈)

non-derivatized

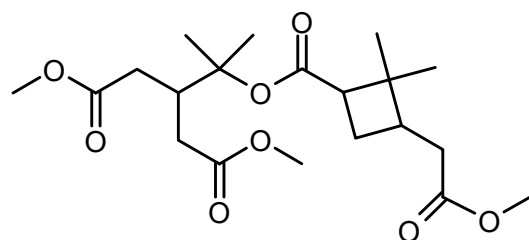


or

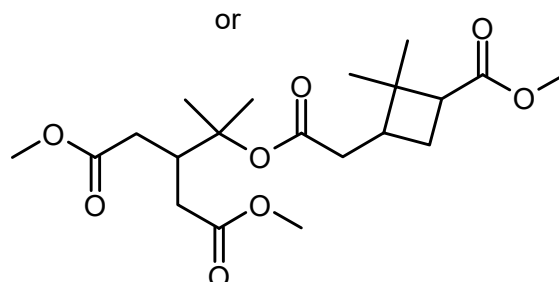


(a)

methylated MW 400 (C₂₀H₃₂O₈)



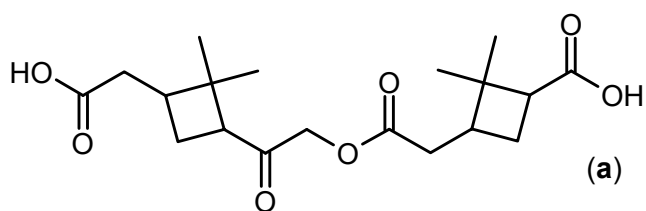
or



(b)

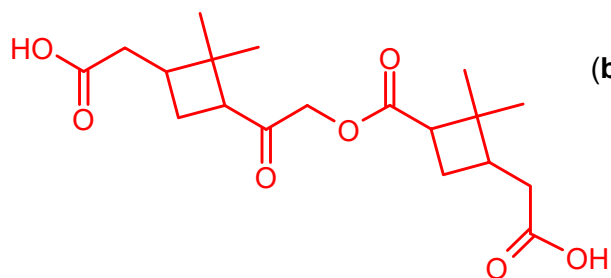
MW 368 (C₁₉H₂₈O₇)

non-derivatized



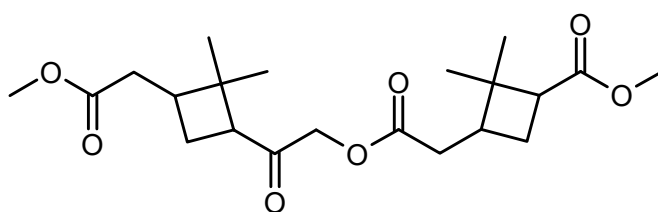
(a)

or

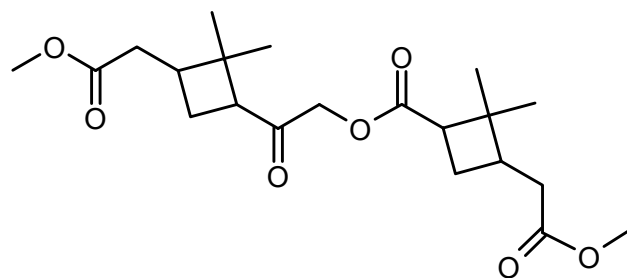


(b)

methylated MW 396 (C₂₁H₃₂O₇)



or



566

567 **Fig. 1.** Overview of the proposed high-molecular-weight ester compounds present in α -pinene/O₃ SOA which
568 were investigated in the present study. The compounds present in underivatized α -pinene/O₃ SOA are
569 highlighted in red color.

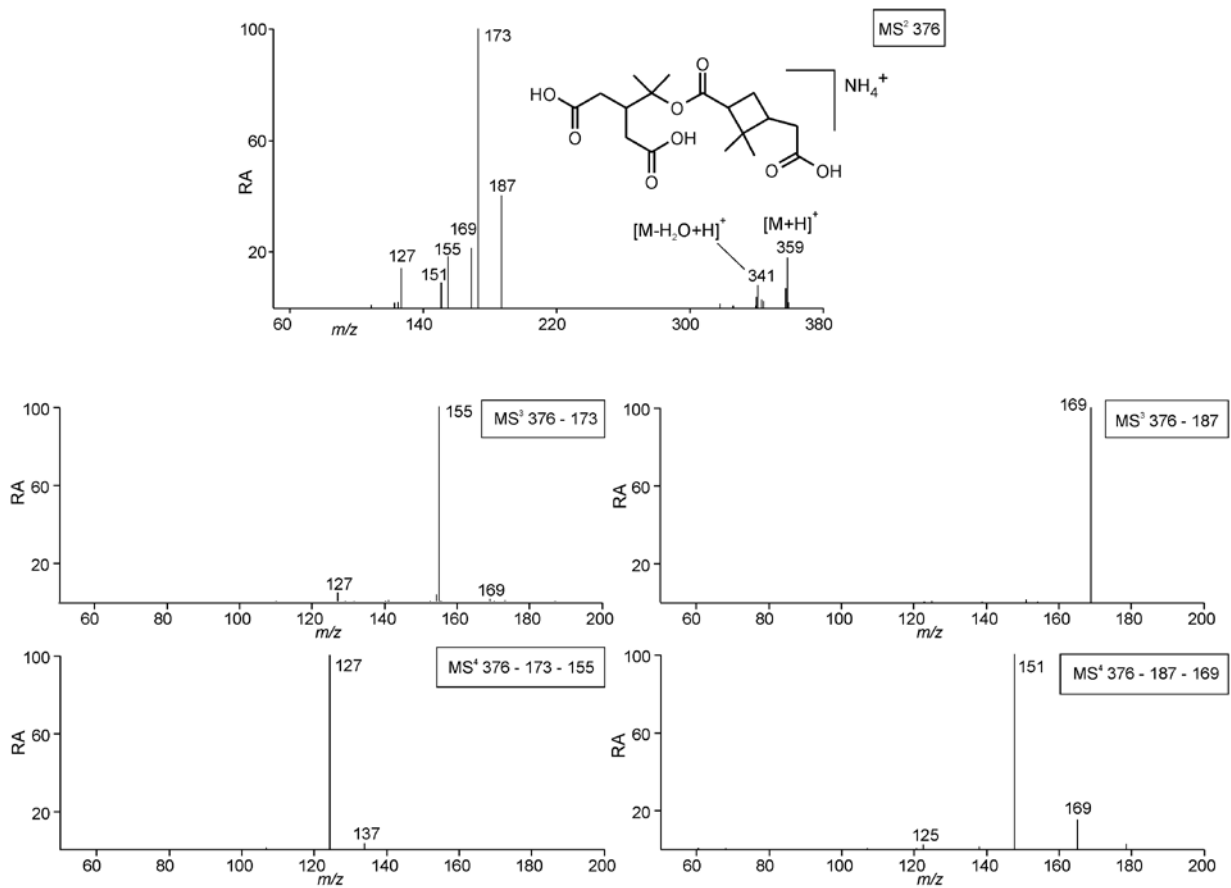


Fig. 2. Selected LC/(+)ESI-MS data for the non-derivatized MW 358 compound eluting at 24.7 min (Fig. S3) with its proposed structure in α -pinene/O₃ SOA, showing the MS² data for its ammonium adduct ion at m/z 376, m/z 376 \rightarrow m/z 173 MS³ data, m/z 376 \rightarrow m/z 173 \rightarrow m/z 155 MS⁴ data, m/z 376 \rightarrow m/z 187 MS³ data, and m/z 376 \rightarrow m/z 187 \rightarrow m/z 169 MS⁴ data.

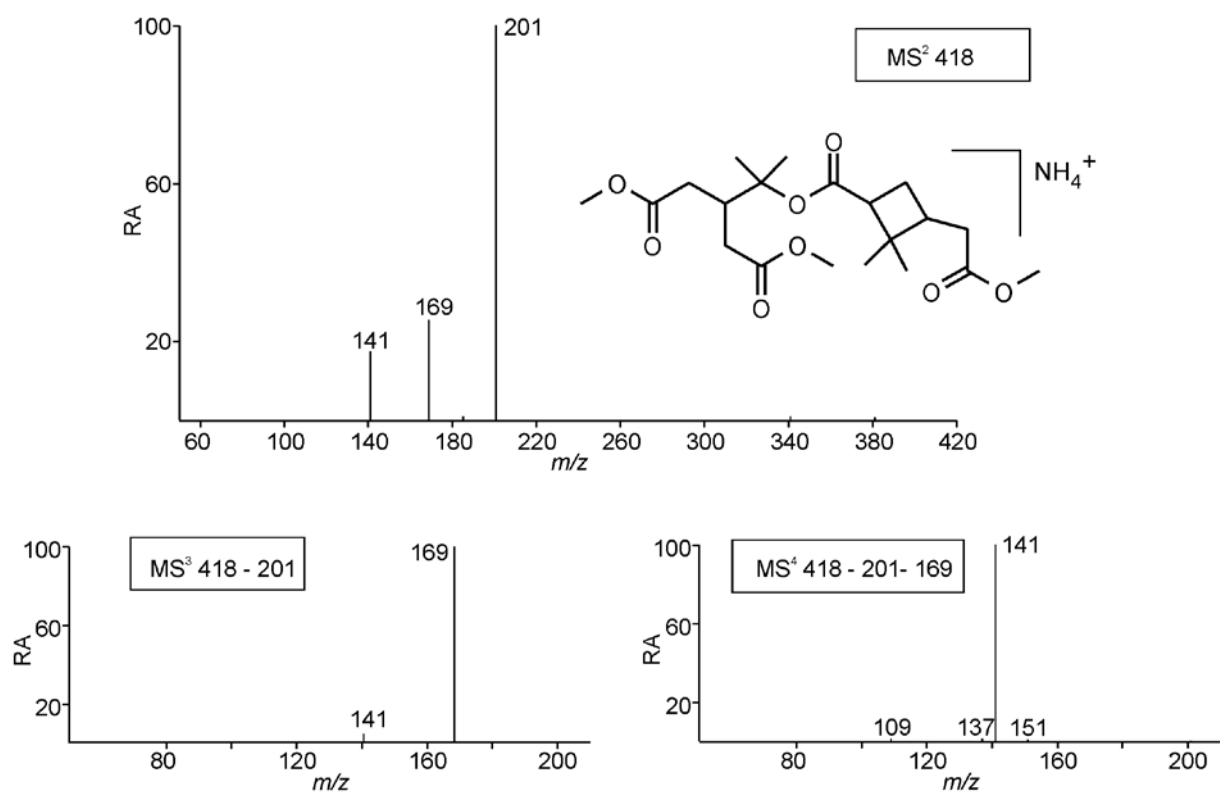


Fig. 3. Selected LC/(+)ESI-MS data for the trimethylated MW 358 compound eluting at 28.0 min (Fig. S4) with its proposed structure in α -pinene/ O_3 SOA, showing the MS² data for its ammonium adduct ion at m/z 418, m/z 418 \rightarrow m/z 201 MS³ data, and m/z 418 \rightarrow m/z 201 \rightarrow m/z 169 MS⁴ data.

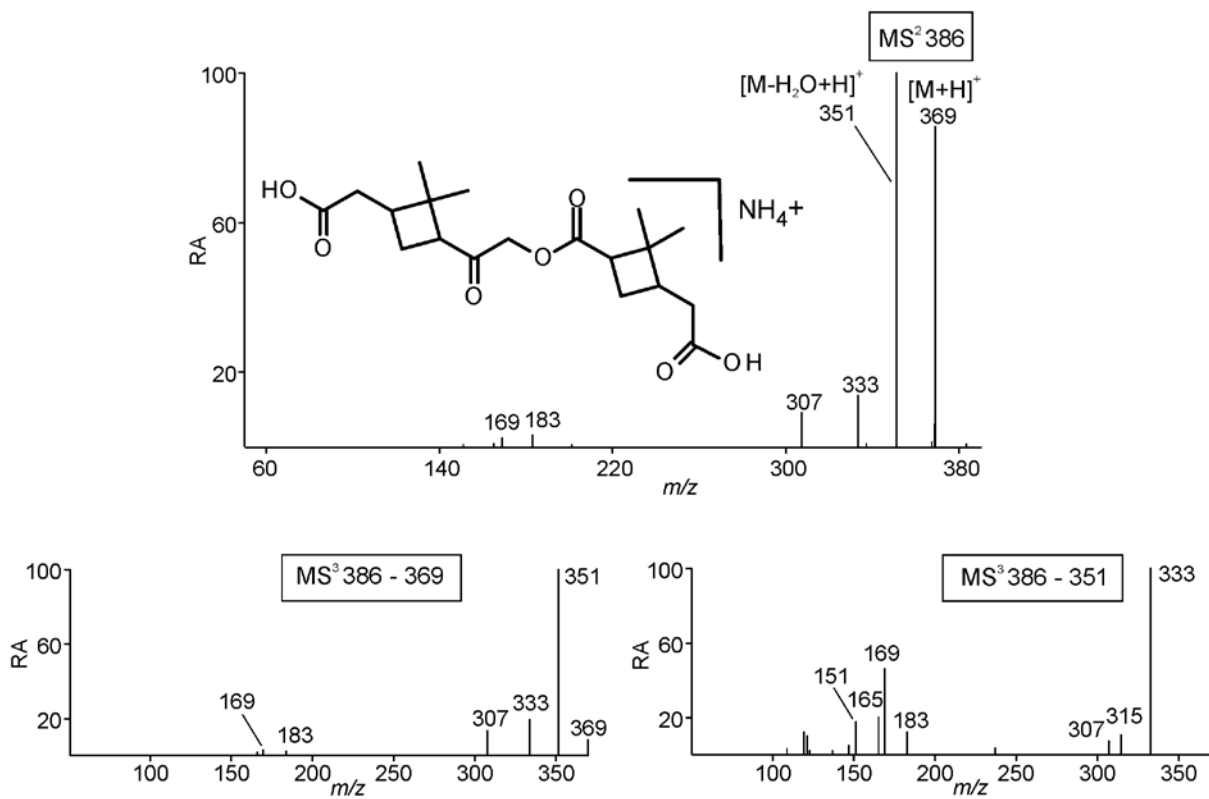


Fig. 4. Selected LC/(+)ESI-MS data for the non-derivatized MW 368 compound eluting at 25.9 min (Fig. S3) with its proposed structure in α -pinene/O₃ SOA, showing the MS² data for its ammonium adduct ion at m/z 386, m/z 386 \rightarrow m/z 369 MS³ data and m/z 386 \rightarrow m/z 351 MS³ data.

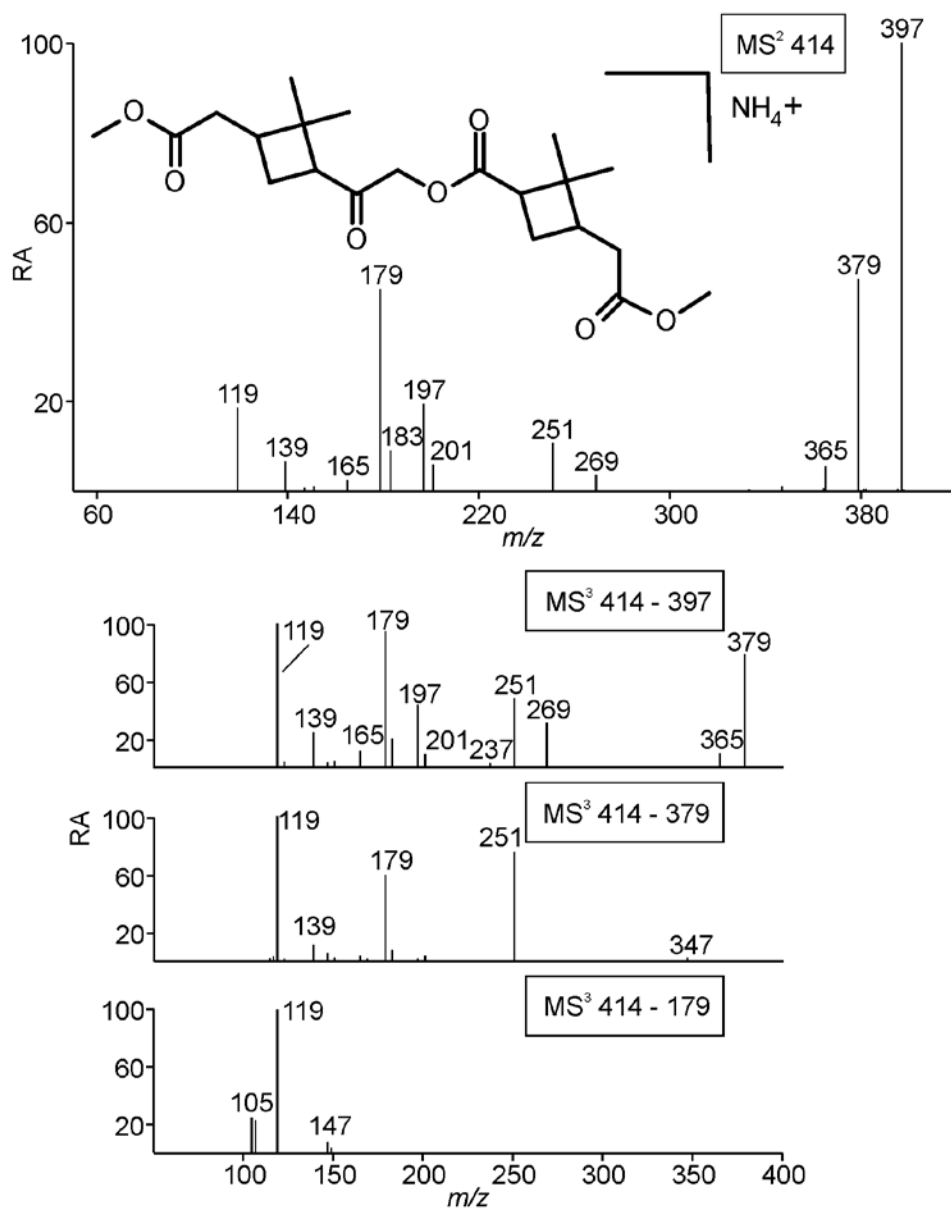
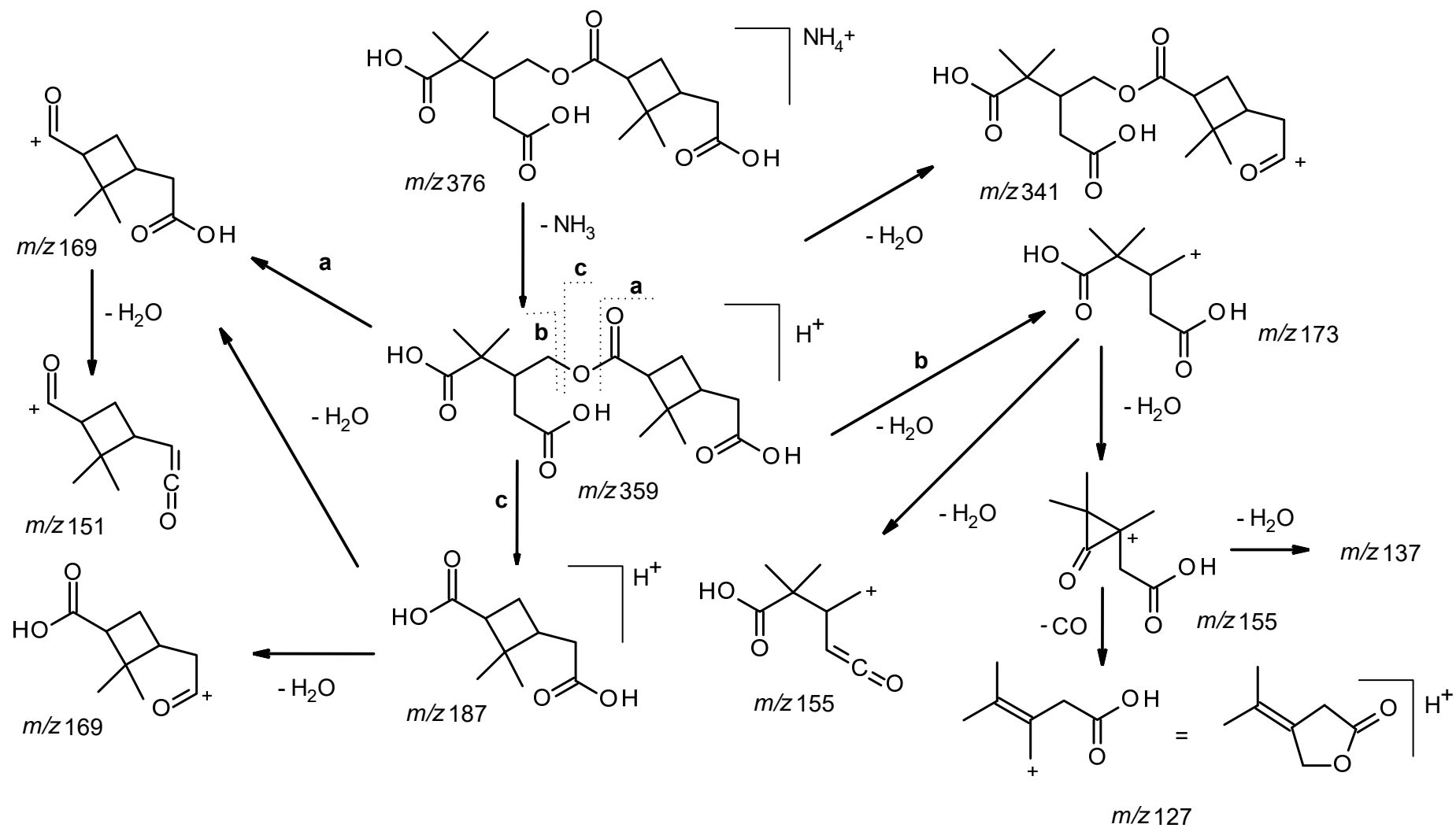
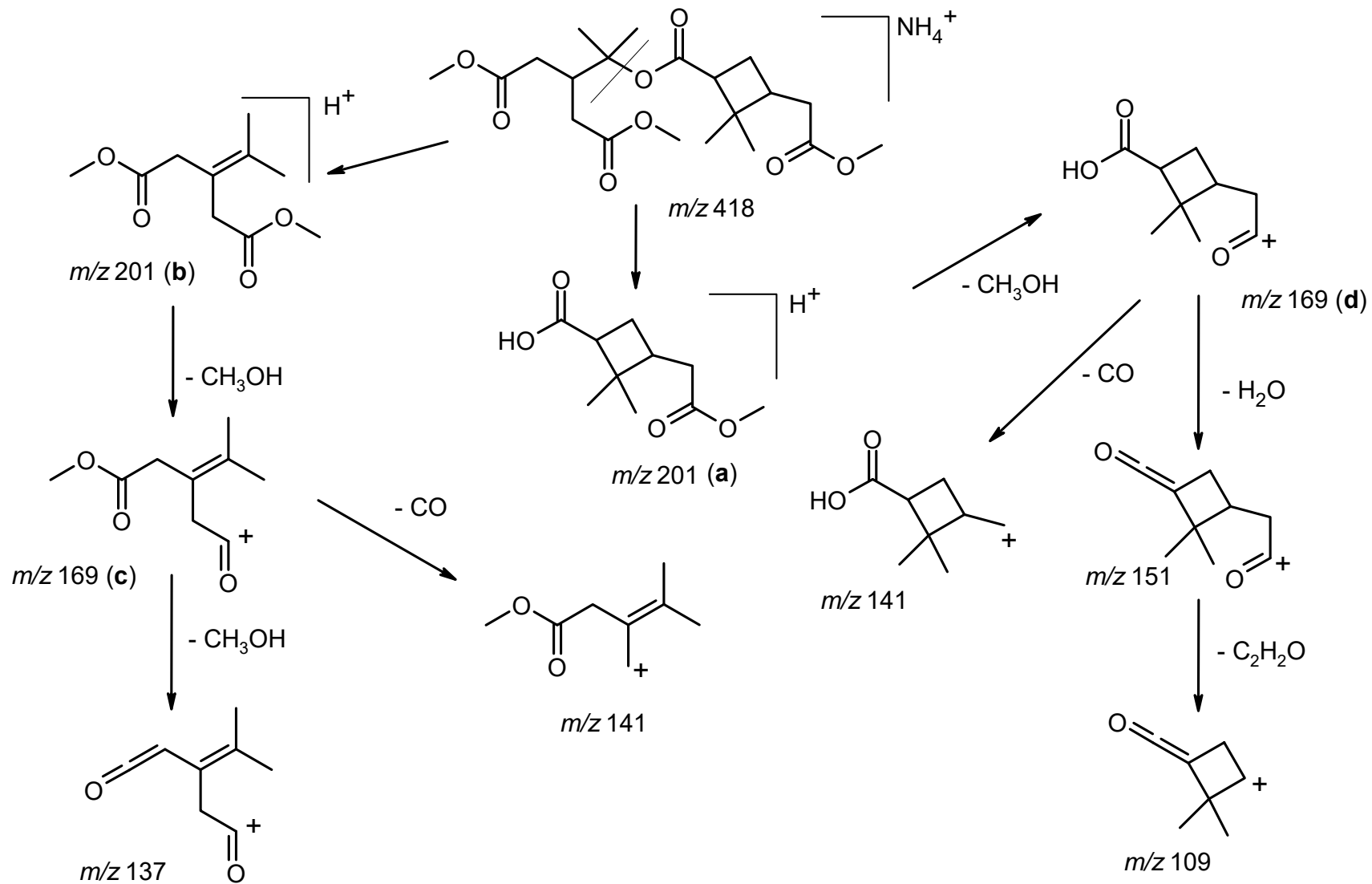


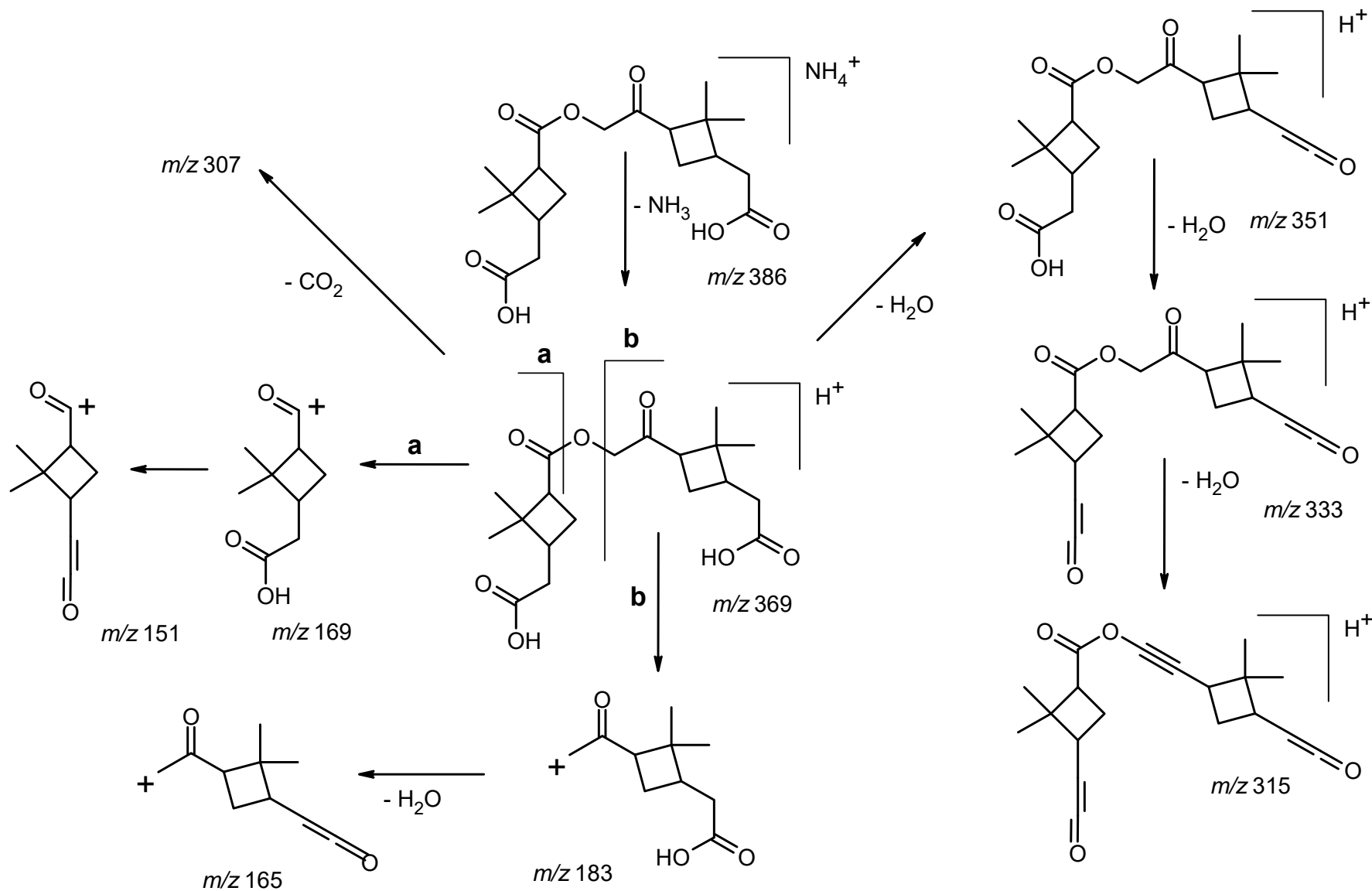
Fig. 5. Selected LC/(+)ESI-MS data for the dimethylated MW 368 compound eluting at 28.4 min (Fig. S4) with its proposed structure in α -pinene/ O_3 SOA, showing the MS^2 data for its ammonium adduct ion at m/z 414, m/z 414 \rightarrow m/z 397 MS^3 data, m/z 414 \rightarrow m/z 379 MS^3 data, and m/z 414 \rightarrow m/z 179 MS^3 data.



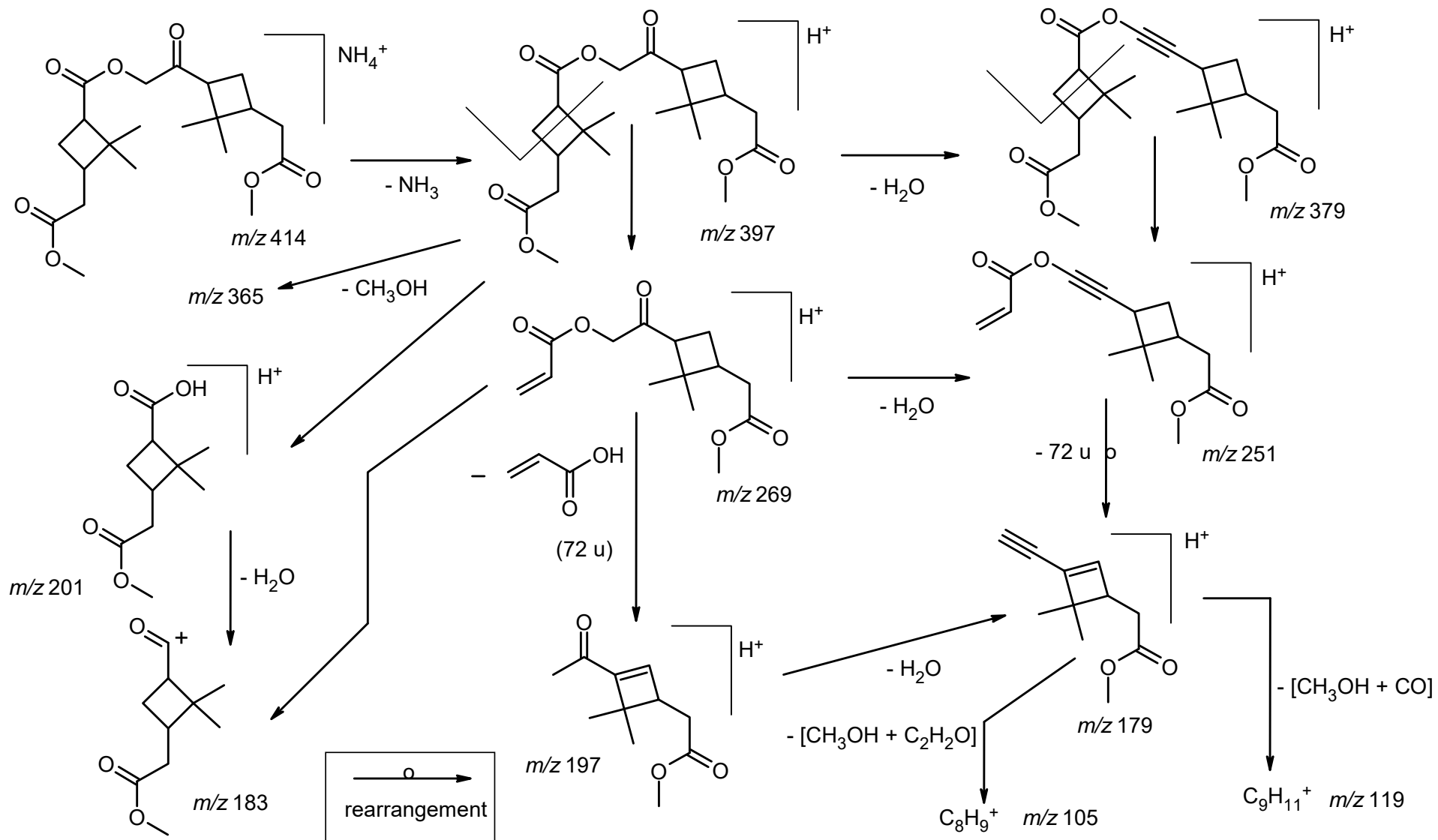
Scheme 1. Proposed fragmentation mechanism for the ammoniated non-derivatized MW 358 ester present in α -pinene/ O_3 SOA.



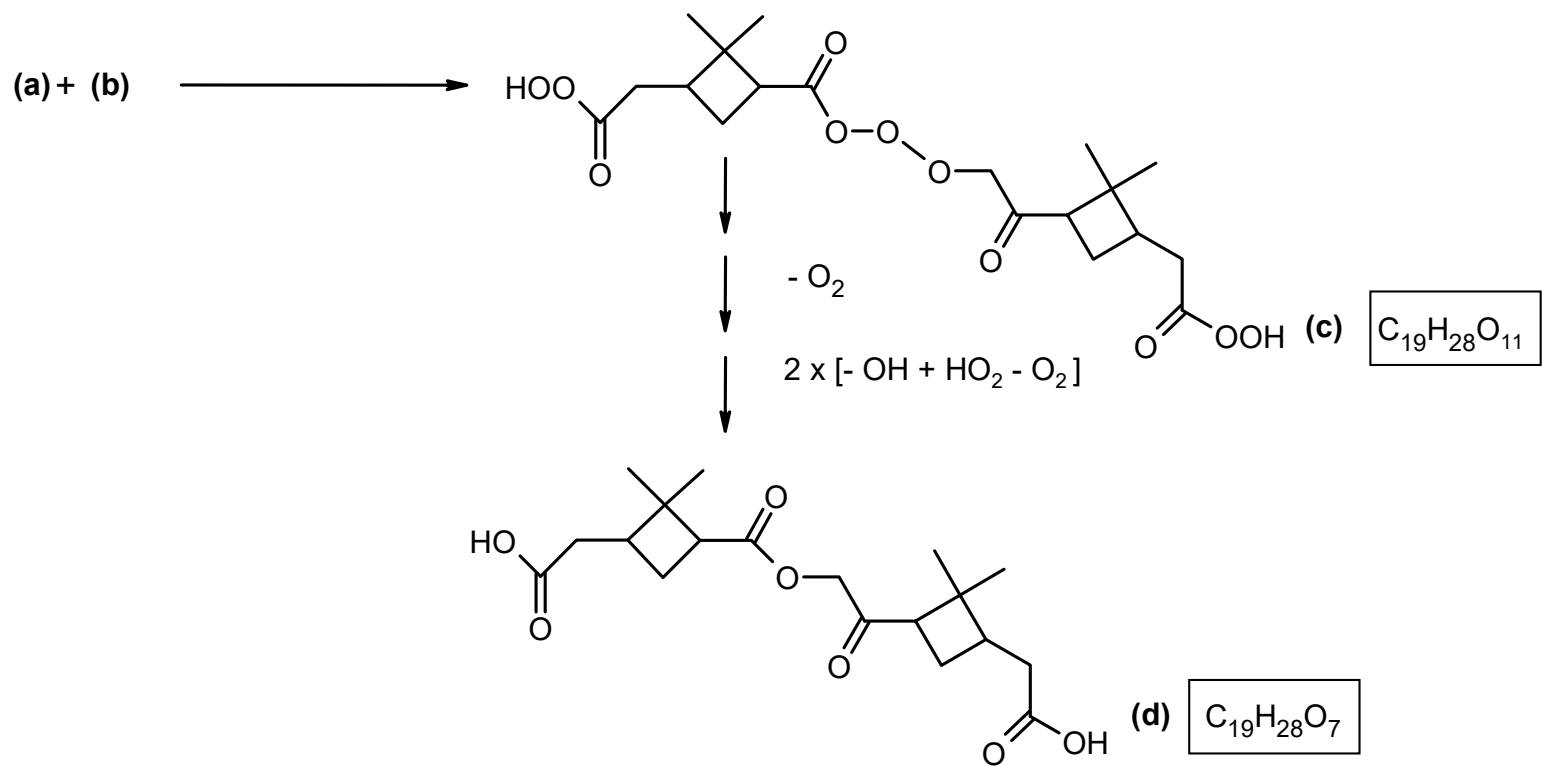
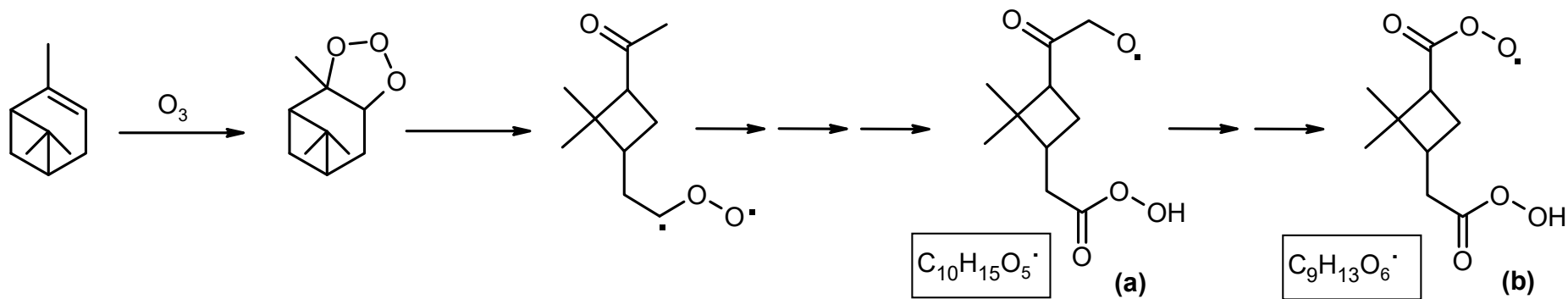
Scheme 2. Proposed fragmentation mechanism for the ammoniated MW 358 ester trimethylated derivative.



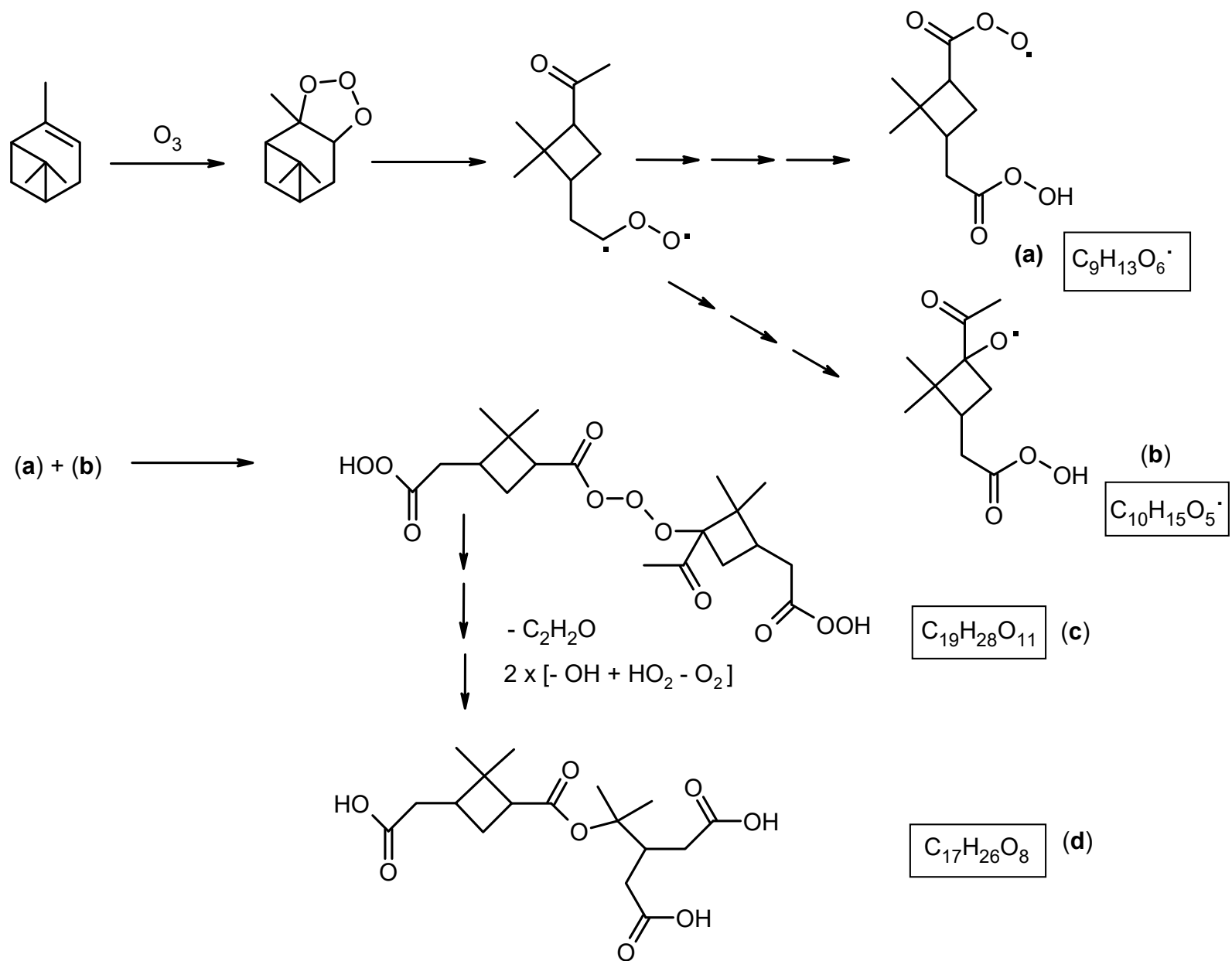
Scheme 3. Proposed fragmentation mechanism for the ammoniated non-derivatized MW 368 ester present in α -pinene/ O_3 SOA.



Scheme 4. Proposed fragmentation mechanism for the ammoniated MW 368 ester dimethylated derivative.



Scheme 5. Proposed simplified mechanism leading to the formation of the MW 368 ester with structure **(b)** (Fig. 1). The mechanisms suggested for the formation of the alkoxy radical related to 7-hydroxypinonic acid **(a)** and the acyl peroxy radical related to *cis*-pinic acid **(b)** are provided in Scheme S4 of the supplement. It is proposed that the latter radicals serve as key intermediates. Radical termination according to a $\text{RO}_2\cdot + \text{R}'\text{O}\cdot \rightarrow \text{RO}_3\text{R}'$ reaction results in a HOM with a molecular composition of $\text{C}_{19}\text{H}_{28}\text{O}_{11}$ **(c)**, a major gas-phase species upon α -pinene ozonolysis which has been detected by CI-APi-TOF MS (Ehn et al., 2012, 2014; Krapf et al., 2016). Further degradation of the labile inner part containing a linear trioxide bridge through the loss of oxygen and conversion of the acyl hydroperoxide groups to carboxyl groups results in the MW 368 ester.



Scheme 6. Proposed simplified mechanism leading to the formation of the MW 358 ester with structure **(a)** (Fig. 1). The mechanisms suggested for the formation of the acyl peroxy radical related to *cis*-pinic acid **(a)** and the alkoxy radical related to 5-hydroxypinonic acid **(b)** are provided in Scheme S4 of the supplement. It is proposed that the latter radicals serve as key intermediates. Radical termination according to a $\text{RO}_2\cdot + \text{R}'\text{O}\cdot \rightarrow \text{RO}_3\text{R}'$ reaction results in a HOM with a molecular composition of $\text{C}_{19}\text{H}_{28}\text{O}_{11}$ **(c)**, a major gas-phase species upon α -pinene ozonolysis which has been detected by CI-APi-TOF MS (Ehn et al., 2012, 2014; Krapf et al., 2016). Further degradation of the labile inner part containing a linear trioxide bridge through the loss of ketene and conversion of the acyl hydroperoxide groups to carboxyl groups results in the MW 358 ester.